

Article

# Preparation of a Zirconia-Based Ceramic Membrane and Its Application for Drinking Water Treatment

Mohamed Boussemghoune <sup>1,\*</sup>, Mustapha Chikhi <sup>1</sup>, Fouzia Balaska <sup>1</sup>, Yasin Ozay <sup>2</sup>, Nadir Dizge <sup>2</sup> and Brahim Kebabi <sup>3</sup>

<sup>1</sup> Department of Environmental Engineering, University Salah Boubnider Constantine 3, New City Ali Menjeli, Constantine 25000, Algeria; mustapha.chikhi@univ-constantine3.dz (M.C.); fouzia.chikhi@univ-constantine3.dz (F.B.)

<sup>2</sup> Department of Environmental Engineering, Mersin University, Mersin 33343, Turkey; yozay@mersin.edu.tr (Y.O.); ndizge@mersin.edu.tr (N.D.)

<sup>3</sup> Chemical Department, University Mentouri Constantine 1, Constantine 25000, Algeria; brahim.kebabi@umc.edu.dz

\* Correspondence: mohamed.boussemghoune@univ-constantine3.dz

Received: 20 April 2020; Accepted: 6 May 2020; Published: 3 June 2020



**Abstract:** This work concerns the preparation of a mineral membrane by the slip casting method based on zirconium oxide ( $ZrO_2$ ) and kaolin. The membrane support is produced from a mixture of clay (kaolin) and calcium carbonate (calcite) powders using heat treatment (sintering). Membrane and support characterization were performed by Scanning Electron Microscopy (SEM), X-ray Fluorescence (XRF), Fourier Transform Infrared Spectroscopy (FTIR), X-ray Diffraction (XRD), and Raman Spectroscopy. The prepared mineral membrane was tested to treat drinking water obtained from different zones of the El Athmania (Algeria) water station (raw, coagulated, decanted, and bio filtered water). Experimental parameters such as permeate flux, turbidity, and total coliforms were monitored. The results showed that the mineral membrane was mainly composed of  $SiO_2$  and  $Al_2O_3$  and the outer surface, which represented the membrane support, was much more porous than the inner surface where the membrane was deposited. The permeate flux of the raw water decreased with filtration time, due to a rejection of the organic matters contained in the raw water. Moreover, the absence of total coliforms in the filtrate and the increase in concentration in the concentrate indicate that the prepared mineral membrane can be used for drinking water treatment.

**Keywords:** kaolin; membrane;  $ZrO_2$ ; flux; turbidity; total coliforms

## 1. Introduction

Membrane processes are increasingly used in industrial areas, covering a wide range of operating conditions and module designs. Using membrane technology, instead of a conventional separation or purification step that is part of an existing industrial process, can reduce overall energy consumption and produce acceptable results under softer conditions. In addition, membrane processes generally permit continuous operation and can be combined easily with other separation processes [1–3].

The significant development of membrane filtration processes has generated a great deal of interest in research on membrane materials. Although polymeric membranes have been used in industrial areas for many years, inorganic membranes, also known as ceramic membranes, are used for longer life, considering their better chemical and mechanical stabilities compared to polymeric membranes [4–6]. For this reason, many studies have been performed in recent years to develop new types of inorganic membranes [7,8].

The development of clay-based inorganic membranes can lead to an important new technological application that will add economic value to the enormous natural deposits of clay minerals, many of

which are currently underutilized [9]. Kaolins are white, friable, and refractory clays, consisting mainly of kaolinite of the formula  $\text{Al}_2\text{Si}_2\text{O}_5(\text{OH})_4$  or aluminum silicates ( $\text{Al}_2\text{SiO}_5$ ). It was discovered in China and it is used on the basis of porcelain manufacturing and also in the ceramic industry [10]. Clay (kaolin) is used extensively for the production of microporous tubular supports that can withstand high pressures and chemical attacks, where zirconium oxide gels are deposited for the preparation of membranes [11].

Ceramic membranes (CM) have been used in various industries, such as food, petrochemical, chemical, biotechnological, pharmaceutical, dairy, etc. [12]. So far, many materials such as zeolites,  $\alpha$ - and  $\gamma$ -alumina ( $\text{Al}_2\text{O}_3$ ), titania ( $\text{TiO}_2$ ), zirconia ( $\text{ZrO}_2$ ), silicon oxide ( $\text{SiO}_2$ ), and microporous glasses are commonly used in the development of ceramic membranes [13,14]. To date, various methods have been used to prepare inorganic ceramic membranes. These methods include chemical extraction, the sol-gel method, solid state sintering, phase separation, chemical vapor deposition and synthesis methods [15–17].

Zirconium oxide ( $\text{ZrO}_2$ ) was used to prepare a flexible and thermally stable porous ceramic membrane, using PVdF–HFP as a binder. The membrane showed 60% porosity with good electrolyte uptake, thermal stability of up to 400 °C, and substantial  $\text{Li}^+$ -ion transport number [18]. Ceramic zirconium membranes were used in the separation of oil-in-water emulsion [19,20]. Commercial alumina microfiltration membranes were coated by the nano-sized  $\text{ZrO}_2$  to reduce the membrane fouling by oil droplets. They reported that the modified membrane reached the steady flux in a very short time and the steady flux retained 88% of the initial flux, even when oil rejection was above 97.8% [20]. The oily wastewater produced from the post-treatment unit of the refinery processes was treated using flocculation and a zirconia-based microfiltration membrane (0.2  $\mu\text{m}$ ) [21]. The membrane was operated at a transmembrane pressure of 0.11 MPa and a cross-flow velocity of 2.56 m/s. The membrane filtration results showed that the membrane fouling decreased, and the permeate flux as well as the permeate quality increased with flocculation as pretreatment [21]. In another study, Kroll et al. fabricated and characterized zirconia microtubes with 1.6 and 1.0 mm outer and inner diameters, respectively, for bacteria filtration and digestion [22]. Tubular zirconia membranes sintered with a temperature of 1050 °C had an open porosity of 51.3%, with pore sizes of  $\leq 0.2 \mu\text{m}$ , and were suitable for bacteria filtration [22]. Commercial tubular zirconia membranes supported on the alumina were used for modification with two different grafting procedures [23]. Different kinds of hydrophobic ceramic membranes were prepared by grafting organosilane molecules (FAS) on the membrane surface. The hydrophobic ceramic membranes with 200 and 50 nm pore diameters were used for water desalination by membrane distillation [24]. The zirconia membrane was prepared using an in situ hydrothermal crystallization technique for the separation of methyl orange dye [25]. The porosity, average pore size and pure water permeability of the zirconia membrane were estimated to be 42%, 0.66  $\mu\text{m}$ , and  $1.44 \times 10^{-6} \text{ m}^3/\text{m}^2 \text{ s kPa}$ , respectively. The prepared membrane showed a 61% rejection of methyl orange from the aqueous solution and a high permeation flux of  $2.28 \times 10^{-5} \text{ m}^3/\text{m}^2 \text{ s}$  at 68 kPa operating pressure [25]. The zirconia-based ceramic composite membranes were used for the separation of whey components [26]. The prepared membrane enhanced relatively high protein content (~80%) and low lactose retention (~7%), with a 40  $\text{L}/\text{m}^2\text{h}$  permeate flux value. A zirconia ultrafiltration (UF) membrane with a mean pore diameter of 40 nm was prepared in single step coating of zirconia nanopowder suspension by the slip casting method [27]. The membrane was applied for treatment of industrial (tannery) and domestic (kitchen sink) wastewater. They reported that 82% and 92% removal of chemical oxygen demand (COD) were obtained for tannery wastewater and kitchen sink wastewater, respectively. Turbidity was reduced below 1 NTU for both the effluents, with complete removal of pathogenic organisms [27].

In this study, an inexpensive tubular zirconia membrane on a low cost porous ceramic support was synthesized and characterized. Kaolin powders were used to prepare the membrane support.  $\text{CaCO}_3$  and Methocel were used in the support preparation as inorganic and organic additives, respectively. The prepared ceramic membrane and support were characterized by SEM, XRF, FTIR,

XRD, and Raman Spectroscopy. The membrane was used to remove organic matters from drinking water. The developed ceramic membrane was also tested for removal of *Escherichia coli* (*E. coli*). Variations in the permeate flux of distilled and raw drinking water versus filtration time were investigated. Moreover, the characterizations of raw drinking water, permeate and concentrate quality were also illustrated.

## 2. Material and Methods

### 2.1. Characterization of Raw Kaolin Powders

Table 1 shows the chemical composition of the raw kaolin determined by X-ray fluorescence (XRF) analysis. A chemical composition of kaolin powders for the ceramic membrane support showed that  $\text{SiO}_2$ ,  $\text{Al}_2\text{O}_3$ ,  $\text{Fe}_2\text{O}_3$  were major elements. However,  $\text{K}_2\text{O}$ ,  $\text{Na}_2\text{O}$ ,  $\text{MgO}$ ,  $\text{P}_2\text{O}_5$ ,  $\text{TiO}_2$ , and  $\text{MnO}$  were detected as minor elements.

**Table 1.** Chemical analysis (wt. %) of the raw kaolin.

Oxide	Weight (%)
$\text{SiO}_2$	55.080
$\text{Al}_2\text{O}_3$	29.041
$\text{Fe}_2\text{O}_3$	2.813
$\text{K}_2\text{O}$	1.422
$\text{Na}_2\text{O}$	0.320
$\text{MgO}$	0.172
$\text{CaO}$	0.010
$\text{P}_2\text{O}_5$	0.082
$\text{TiO}_2$	0.066
$\text{MnO}$	0.014
Loss on ignition	10.980

### 2.2. The Methods of the Membrane Support and Ceramic Membrane Preparation

In this part, we describe the methods of the membrane support from the clay powders (kaolin) and zirconia-based ceramic membrane preparations. The clay consisted mainly of aluminum silicate ( $\text{Al}_2\text{SiO}_5$ ), intended for the manufacture of the tubular microporous support. The method of tubular support preparation can be summarized in the following steps [28,29]:

- Thermal treatment of the clay material at a temperature of 400–600 °C for 30 min for the removal of water contained in kaolin (dehydration) and the combustion of organic matters.
- Grinding of the clay material to obtain small particles.
- Sieving of the small particles to obtain particles smaller than 125  $\mu\text{m}$ .
- Addition of kaolin (75%) and calcium carbonate ( $\text{CaCO}_3$ ) (22%) for the appearance of pores with an acceptable number and size in the final support.
- Addition of an organic additive (Methocel) (3%) to improve the elastic properties of the dough and to facilitate the formation process.
- Mixing of the above-mentioned materials with the presence of the solvent (distilled water), by using the mixer until a paste of good elastic properties was obtained. Then, the mixture was placed in a tightly closed plastic bag for 12 h to properly spread the water in the ceramic paste.
- Extrusion of ceramic paste in tubular form.
- Drying of the tubular support with ambient air by placing it on the machine containing the rotating cylinders to dry it uniformly and maintain its shape for 24 h.

- Sintering the components of the ceramic paste that forms the support at a temperature equal to 1100 °C, which will convert it to anorthite according to a series of reactions during a specific thermal program.

The sintering of the support was realized in the following steps. First, the temperature of the chamber was increased from the ambient temperature to the temperature of 250 °C, with a rise speed of 3 °C/min and a plateau of 15 min. During this step, water could be eliminated quickly. Second, the temperature was increased from 250 to 1100 °C with a rise speed of 3 °C/min and a plateau of 60 min. During this step, organic matters could be removed (Figure 1).

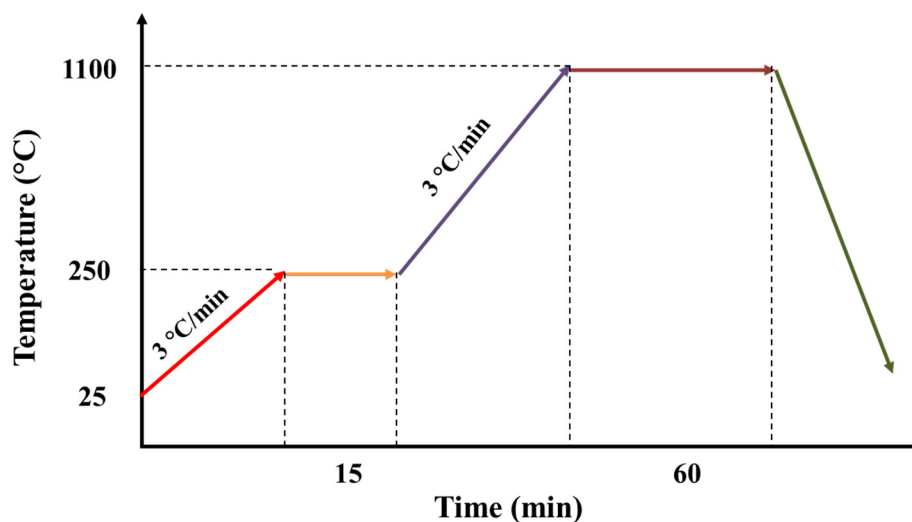


Figure 1. Thermal program used for the sintering of the support.

### 2.3. The Method of the Slip Casting Membrane Preparation

The method consisted of suspending zirconia and polyvinyl alcohol in distilled water and pouring the produced slip inside the porous support (Figure 2). The method results in the controlled diffusion process, which amounts to a simple loss of water from the suspension in the mass of the support; this causes the accumulation of zirconia particles on its surface. The support sintered with thermal sequences ensures that the material can withstand high pressures and chemical attacks. However, zircon oxide ( $ZrO_2$ ) accumulated in the inner part of the tubular support provides the formation of selective permeable membrane.

The method of zirconia-based ceramic membrane preparation can be summarized in the following steps:

- Take 70% of the distilled water and add in 4% by weight of  $ZrO_2$  powder to mix the mixture until a good homogeneous mixture was obtained.
- Place the mixture in an ultrasonic bath for 10 min to dispel the granules and dissolve the sediments.
- Then, add 26% polyvinyl alcohol (PVA) and mix for 12 h to obtain the suspension solution.
- The solution is poured into the support for 10 min and dried for 5 min.

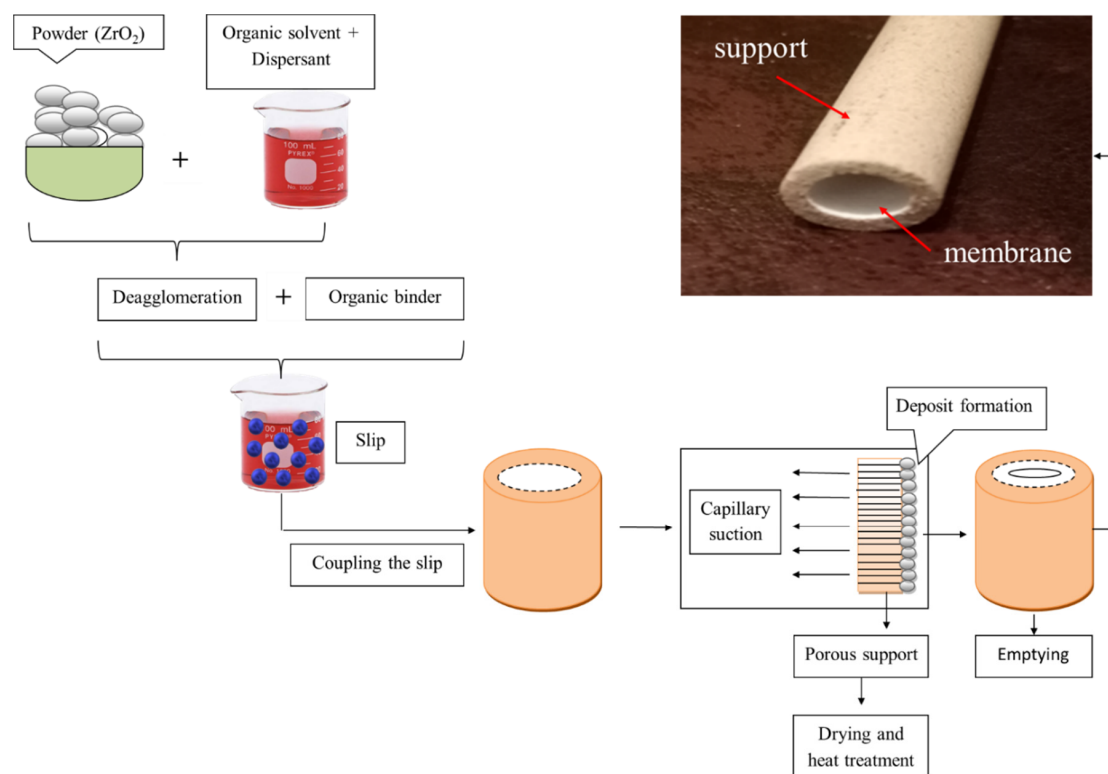


**Figure 2.** The method for preparing the slip casting membrane.

#### 2.4. Experimental Setup of Filtration

The prepared zirconia-based ceramic membrane was used for the treatment of drinking water obtained from Oued El Athmania water treatment plant (Mila, Algeria). The filtration experiments were carried out using a tangential filtration system (Figure 3). The total volume of the reservoir was 5 L, and 3 L of drinking water was used for each experiment. The effective membrane area was 45 cm<sup>2</sup> and cross-flow velocity was 4.18 m/s. The concentrate was recycled back into the feed tank and the filtered water (permeate) was collected in an Erlenmeyer flask for analysis. The volume of filtrate was monitored as a function of time to determine the permeate flux ( $J_p$ ).

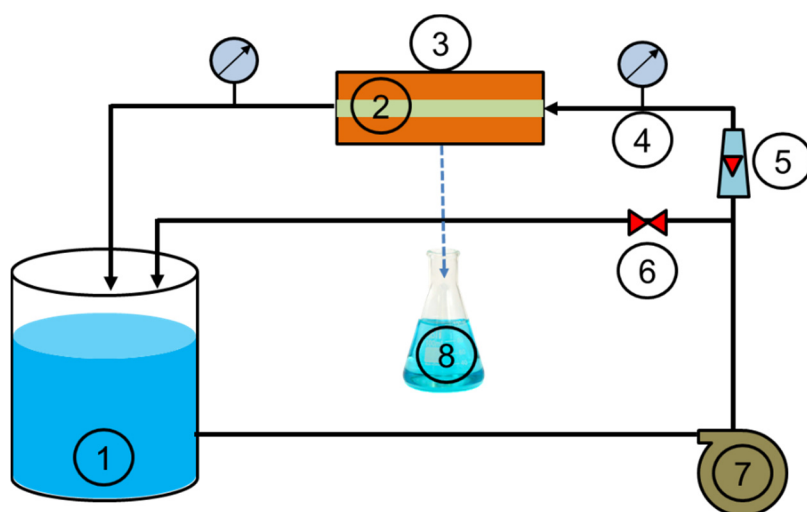


**Figure 3.** Experimental setup of the tangential filtration system (reservoir (1), tangential membrane (2), module (3), pressure gauge (4), flowmeter (5), valve (6), pump (7), permeate (8)).

### 2.5. Determination Method of Total Coliform Bacteria

Coliform bacteria filtration experiments were also carried out by prepared ceramic membrane. Coliform bacteria in water, thermo-tolerant coliforms, and *E. coli* were investigated and counted using the most probable number (MPN) technique in liquid medium. BCP (Bromocresol Purple) Lactose Broth Tubes were used for presumptive identification and enrichment of total coliforms, including thermotolerant coliforms. Water samples were collected in sterile glass bottles (1 L) in order to detect and count the final concentration of bacteria after filtration. The final reading was carried out according to the requirements of the MPN table, taking into account that *E. Coli* is a producer of gas and indole at 44 °C.

## 3. Results

### 3.1. Characterization of the Support and Zirconia-Based Ceramic Membrane

The characterizations of the support and zirconia-based ceramic membrane are given in Tables 2 and 3.

**Table 2.** The characteristics of the tubular kaolin support.

Properties	Support Material
Outside diameter	9 mm
Inside diameter	4.6 mm
Thickness	2.2 mm
Length	190 mm
Operating pH range	1–14
Washing pH range	1–14

**Table 3.** The characteristics of the tubular zirconia-based ceramic membrane.

Properties	Ceramic Membrane
Total area	$4.48 \times 10^{-3} \text{ m}^2$
Average pore diameter	0.2 $\mu\text{m}$
Operating pH range	1–14
Washing pH range	1–14

#### 3.1.1. Scanning Electron Microscopy (SEM)

Scanning Electron Microscopy allows for the observation of the morphology and cavities of the membrane-support (inner and outer surfaces). It should be remembered that the slip casting membrane was deposited inside the tubular support. Figure 4A,B show the outer surface of the support material. It could be seen from the figures that there were large and irregular pores on the support layer. Figure 4C,D show the inner surface of the ceramic membrane. The layered structure of zirconia and the asymmetric distribution of the pores can be seen from the figures. Moreover, cross-section images of the tubular membrane are seen in Figure 4E,F. The outer surface of the support had wider cavities compared to the inner surface. These cavities can be considered to be an advantage for deposition or adhesion of the solution inside the module.

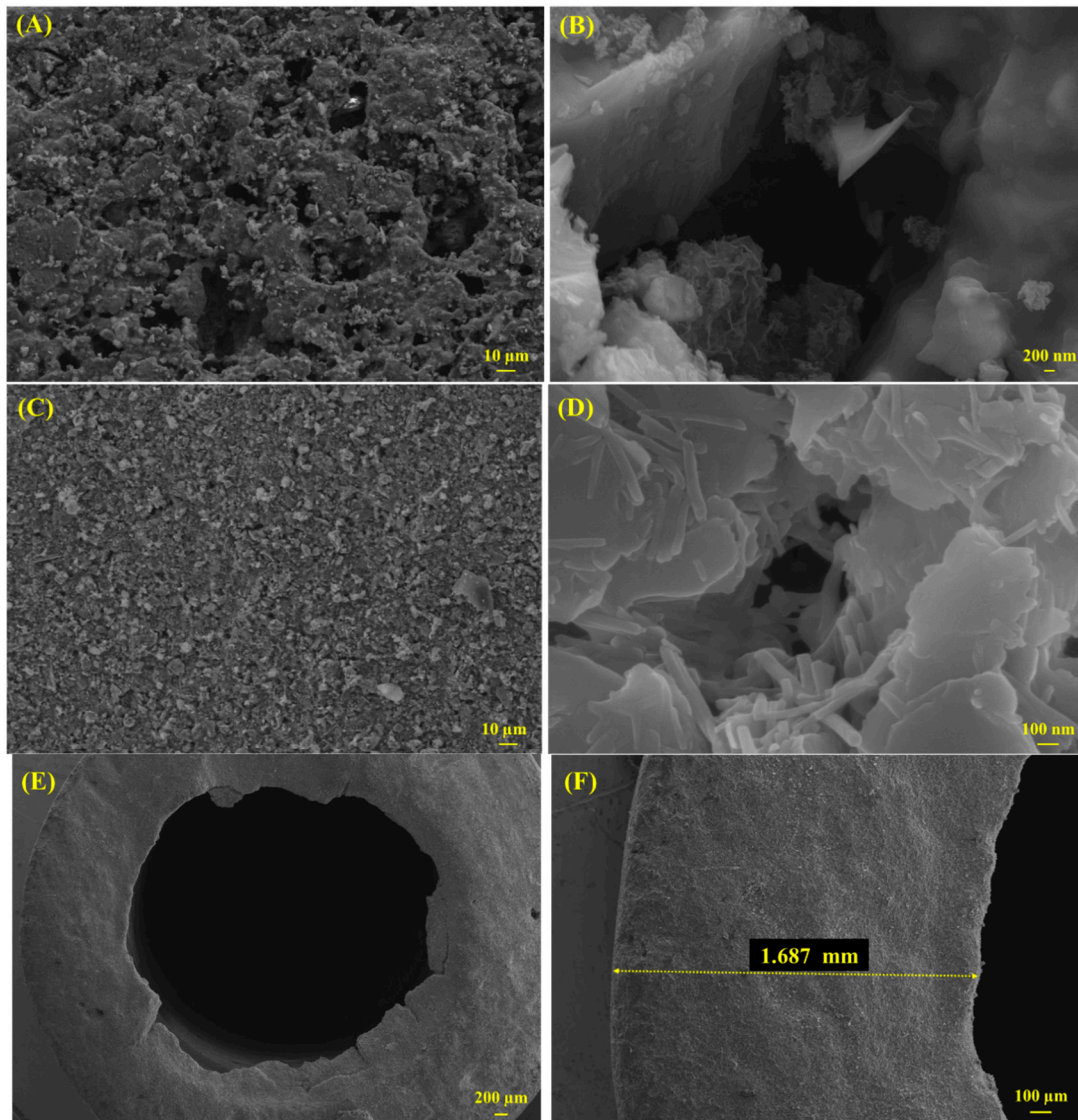


**Figure 4.** SEM images of the support and ceramic membrane (A,B): the outer surface of the support material; (C,D): the inner surface of the ceramic membrane; (E,F): cross-section of the tubular membrane.

### 3.1.2. X-ray Fluorescence (XRF)

The X-ray fluorescence analyses were carried out by a Panalytical Epsilon 3 spectrophotometer, for the evaluation of the most present elements in the membrane support. This energy dispersive X-ray spectrophotometer was connected to a computer using the Omnian analysis software. The sample was placed under helium flow during the analysis. Fluorescence X-ray spectra were recorded under different excitation conditions.

The use of a particular filter with a potential difference and a particular current allows for the better exploration of a particular region of the spectrum. For the support material, the first spectrum was realized with a potential difference ( $d_p$ ) of 5.00 keV and a current of 1000  $\mu$ A (Figure 5A). It allowed us to explore the region of energies up to about 4 keV. For the zirconia-based ceramic membrane, the second spectrum was realized with a silver filter with a thickness of 100  $\mu$ , a  $d_p$  of 30.00 keV and a current of 300  $\mu$ A (Figure 5B). It allows the peaks of high energy to be observed. However, in this case, the peaks are strongly attenuated. From the spectrograms of Figure 5A,B, excitation energy spectra in the range of 1.486 to 1.597 keV and 1.739 to 1.836 keV corresponding to atoms (Al) and (Si), respectively, come from aluminum silicate ( $Al_2SiO_5$ ) (the clay material). Moreover, in the spectrogram of Figure 5B,

the excitation energy spectrum of 15.744 keV corresponding to the zirconia atom (Zr) constituent of the zirconia oxide ( $ZrO_2$ ) membrane was noted. Zirconia detected in the ceramic membrane showed that zirconia had entered the structure of the support material.

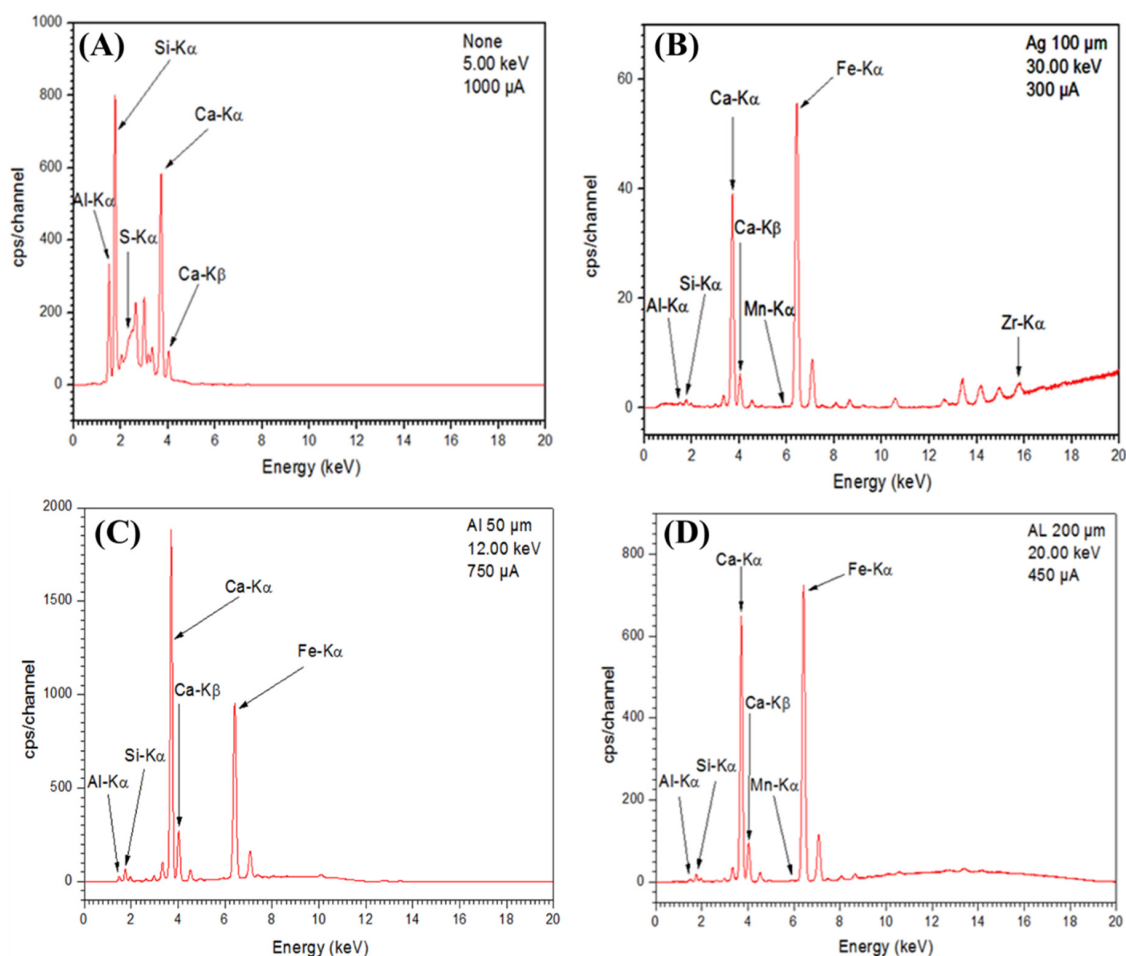


**Figure 5.** X-ray Fluorescence (XRF) spectrum of the support (A,C,D) and ceramic membrane (B).

It was also found from the spectrograms of Figure 5C,D, that the clay used in the preparation of the support contained other constituents such as Mn and Fe. We also noticed excitation energy spectra in the range of 3.5 to 4 keV, which confirmed the presence of the calcium (Ca). It composed the calcium oxide (CaO) by addition of calcite ( $CaCO_3$ ) transformed into (CaO) during the heat treatment of the support paste.

### 3.1.3. X-ray Diffraction (XRD)

The support was characterized by a Panalytical Empyrian brand diffractometer operating under the following conditions: 40 mA, 45 kV with monochromatic radiation  $K_{\alpha} = 1.54 \text{ \AA}$  of copper, equipped with a goniometer and an X-ray detector.

Figure 6 represents XRD reflections of the support at a temperature of 1100 °C for 1 h. The main phase identified in the membrane support was the anorthite ( $CaO, Al_2O_3, 2SiO_2$ ) which was a predominant phase. This phase was very important because of its promising physical and mechanical properties [5,29].

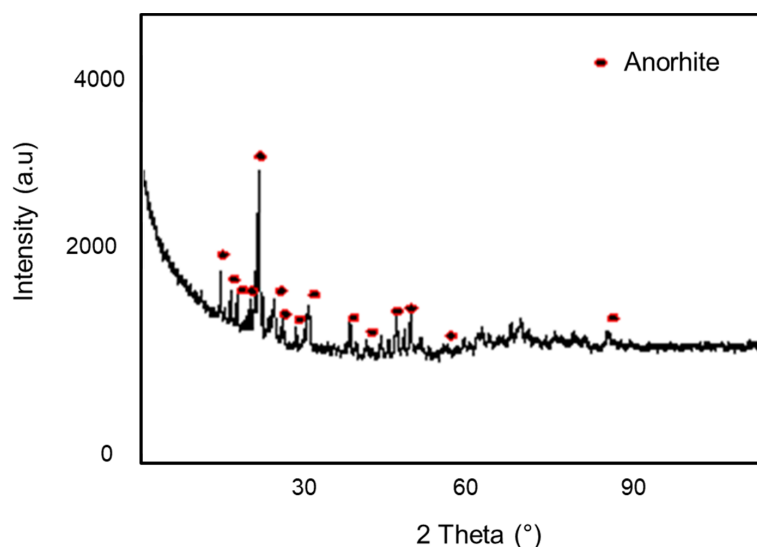


Figure 6. Diffractogram of the clay support.

### 3.1.4. Fourier-Transform Infrared Spectroscopy (FTIR)

Infrared spectra were recorded on a spectrophotometer equipped with an ATR accessory (Jasco FT/IR-4000). Infrared spectroscopy is a tool for mineralogists to characterize the crystallinity of materials, by observing the relative intensities of the hydroxyl (OH) vibration bands and that of the Si-O, Si-O-Si, Al-OH and Al-O in their structures [30,31].

The IR spectrogram of the clay support represented by Figure 7 was divided into two main zones. The first peaks corresponded to high frequency bands (wave numbers) between 3700 and 2800  $\text{cm}^{-1}$ , and the second peaks corresponded to the lower frequencies located in the 1500–500  $\text{cm}^{-1}$  area. The high frequency bands (zone II) concerned the vibration of OH hydroxyls, while the low frequency bands (zone I) related to the Si-O, Si-O-Si, Al-OH-Al, Al-OH, and Al-O bond networks [32].

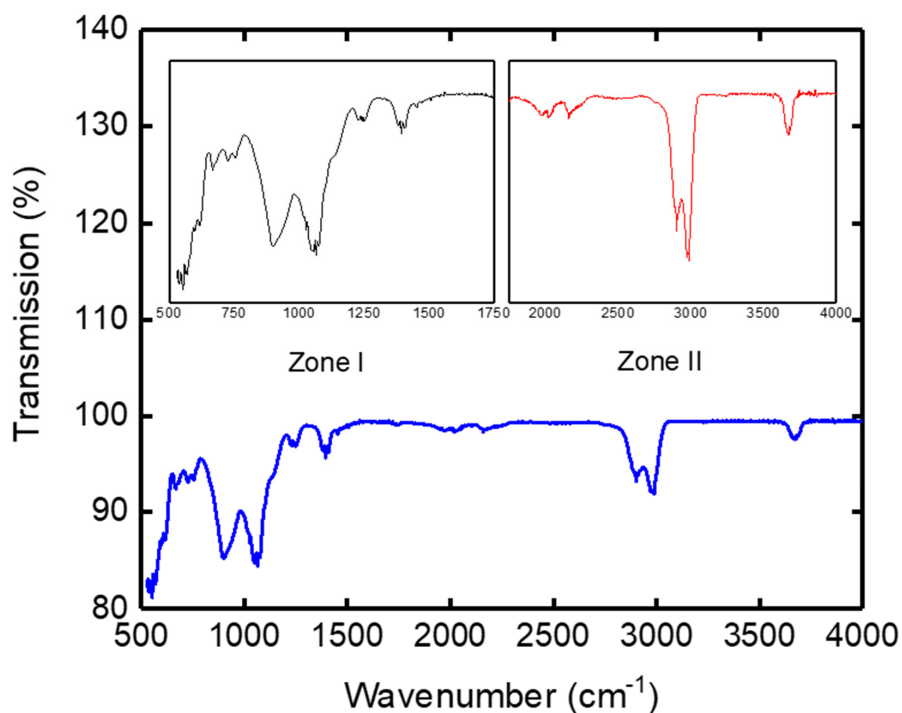


Figure 7. IR spectrogram of the support.

The wave numbers ( $\nu$ ) of peaks and the functional groups corresponding to kaolin are summarized in Table 4. According to Table 2, in correlation with the literature, it was found that the clay used as support contained the different chemical elements with different percentages, such as Si, Al, Fe' and bonds with hydroxyls, which has been confirmed by several authors [33–35].

Table 4. Attribution of vibration bands of IR spectra of clay materials.

Wave Number $\nu$ in ( $\text{cm}^{-1}$ ) of the Clay Support	Wave Number $\nu$ in ( $\text{cm}^{-1}$ ) Observed in Literature	Kaolin Band Assignment
3670	3695 3670	$\nu$ O-H interlayer $\nu$ O-H grain surface
1070	1096 1010–1033	$\nu$ Si-O $\nu$ Si-O-Si
897	875 937 912–915	Al-OH-Fe <sup>3+</sup> $\delta$ Al-OH-Al intern with Feuillet $\delta$ Al-OH-Al external with layer
780 760	800–778 757–700	Si-O of Quartz Al-OH
540	540	Al-O

### 3.1.5. Raman Spectroscopy

The Raman scattering spectra were collected by a Thermo Fisher DXR spectrometer equipped with an optical microscope, a three-grating monochromator (triple additive mode) and a CCD camera detector (Charge Coupled Device). The exciting radiation of a wavelength of 780 nm was delivered by the beam of a NIR diode laser. The beam was focused with a long frontal lens ( $\times 100$  magnification) numerical aperture of 0.9 over 50  $\mu\text{m}$  of the sample surface. The power irradiating the sample was about 10 mW. The scattered retro Raman spectrum was collected in confocal mode to avoid optical artifacts, particularly the signal from the glass slide above the sample cell. The spectral resolution was 1.9  $\text{cm}^{-1}$ , with a precision on the measurement of the best wave number only 1  $\text{cm}^{-1}$ .

Figure 8 represents the Raman spectrum of the clay support, where several bands were observed. We noticed the appearance of new spectra at 1694, 2080, and 3372  $\text{cm}^{-1}$ , which express the vibrations of  $\nu$  (C=O), Si-H, and OH, respectively [36].

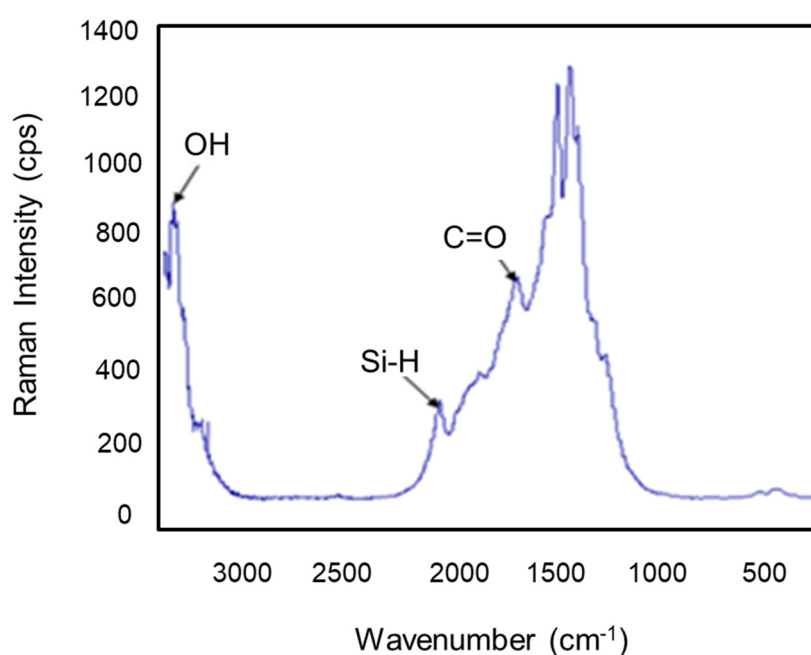
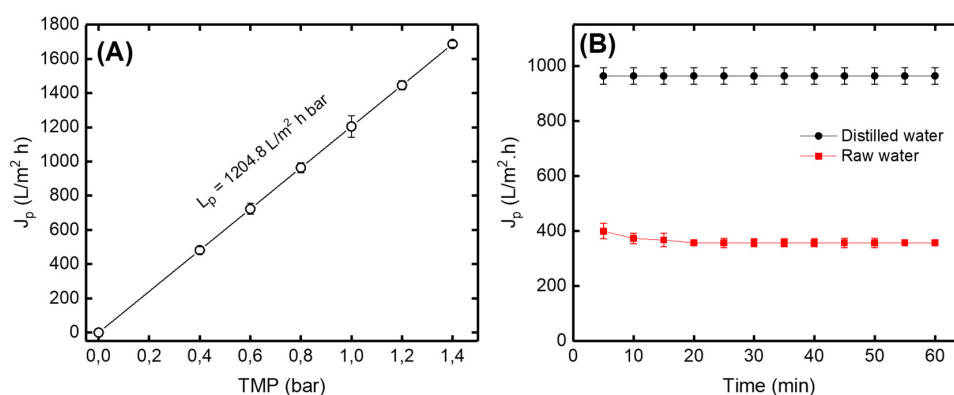


Figure 8. Raman spectrogram of the clay support.

### 3.2. Filtration Experiments

#### 3.2.1. Permeate Flux Variation versus TMP and Time

Figure 9A shows that the permeate flux ( $J_p$ ) of distilled water increases with the increase in the transmembrane pressure (TMP) according to the Darcy law [37]. The variations of the permeate flux ( $J_p$ ) versus time using distilled and raw drinking water are presented in Figure 9B. According to the obtained results, it can be seen that the permeate flux for the distilled and the raw water were not of the same order. This behavior can be explained by the retention of certain matters by the ceramic membrane causing a blockage of the pores, which leads to the reduction of the amount of water passing through the membrane (permeate). The straight line for distilled water explains that the flow of water was constant over the filtration time. On the other hand, the permeate flux of raw drinking water decreased during the first 20 min and then became constant. It could be explained by there being a certain amount of suspended matter which had deposited on the surface of the membrane.



**Figure 9.** (A) Variation of permeate flux ( $J_p$ ) of distilled water versus transmembrane pressure (TMP) (B) Variation of permeate flux of distilled and raw drinking water versus filtration time at TPM = 0.8 bar.

#### 3.2.2. Turbidity Variation Versus Time

Turbidity was determined using a 2100Q portable turbidimeter proposed by Hach, with a tungsten filament lamp equipped with a two-detector ratio optical system for accurate results during routine analyses. It brings greater measurement sensitivity over a wider range of 0 to 1000 NTU. The suspended solid in water causes turbidity. The membrane filtration experiments were carried out for raw drinking water obtained from Oued El Athmania water treatment plant. The turbidity of raw drinking water increased in the concentrate versus filtration time because the water was completely recycled into the feed tank (Figure 10).

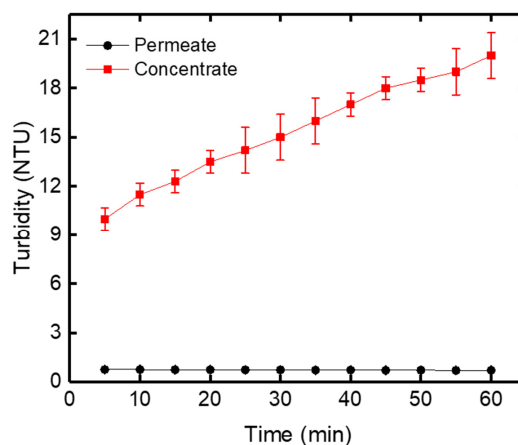


**Figure 10.** Turbidity variation of the permeate and concentrate versus filtration time at TMP = 0.8 bar.

The characterizations of raw drinking water, permeate and concentrate quality are presented in Table 5.

**Table 5.** The properties of raw drinking water, permeate and concentrate.

Physico-Chemical Parameters	Units	Raw Water	Permeate	Concentrate
pH	-	8.35	8.17	8.39
Conductivity	$\mu\text{S/cm}$	1120	1100	1133
Dissolved Salt Rate (DSR)	mg/L	617	610	631
Turbidity	NTU	8.10	0.69	21.10
Total hardness	mg/L	400	380	410
Phosphate ( $\text{PO}_4^{3-}$ )	mg/L	0.07	0.00	0.16
Ammonium ( $\text{NH}_4^+$ )	mg/L	0.03	0.02	0.06
Nitrite ( $\text{NO}_2^-$ )	mg/L	0.0	0.0	0.0
Nitrate ( $\text{NO}_3^-$ )	mg/L	7.00	6.18	7.40
Ferrous iron ( $\text{Fe}^{2+}$ )	mg/L	0.17	0.03	0.33
Manganese ( $\text{Mn}^{2+}$ )	mg/L	0.1	0.0	0.7
Aluminum ( $\text{Al}^{3+}$ )	mg/L	0.0	0.0	0.0
Zinc ( $\text{Zn}^{2+}$ )	mg/L	0.43	0.30	0.60
Chloride ( $\text{Cl}^-$ )	mg/L	177.27	173.72	180.81
Calcium ( $\text{Ca}^{+2}$ )	mg/L	84.17	80.16	92.18

### 3.2.3. Total Coliform Bacteria Variation versus Time

Biological tests of total coliform bacteria were also performed in this work to test the retention capacity of the ceramic membrane. *E. coli* are considered as indicators of the microbial quality of drinking water [38]. In the filtered water (permeate), the number of coliforms was equal to zero during 60 min filtration, which depicted that all of the total coliforms were rejected by the zirconia-based ceramic membrane (Figure 11). On the other hand, in the concentrated water, an increase in the number of total coliforms from 15 to 35 in 100 mL was obtained after 60 min of filtration.

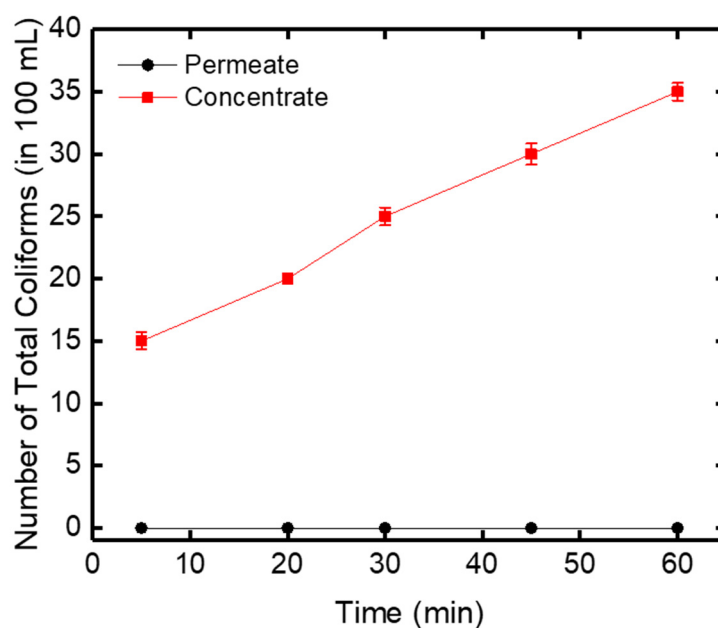


**Figure 11.** Evolution of the number of total coliforms in the permeate and concentrate and versus time.

#### 4. Conclusions

In this work, a zirconia-based ceramic membrane with a tubular configuration was prepared by the casting method. The anorthite support, which had favorable physical and mechanical properties, was prepared by the extrusion method. The inner layer, containing smaller pores compared to the support, reduced the size of the pores and eliminated defects of the support. The membrane filtration results showed that there was an improvement in the physicochemical and bacteriological quality of raw drinking water. The prepared membrane retained all of the total coliforms. Using a ceramic membrane can help to obtain a good clarification, and can reduce the addition of chemical agents such as aluminum and chlorine used for coagulation and disinfection. These agents form an additional pollution, such as the presence of aluminum in the sludge from the settling basin, and an acceptable taste of water after the addition of a smaller amount of chlorine.

**Author Contributions:** This work was carried out by the contribution of all the authors cited in this paper; the author M.B. was interested to the experimental preparation of a Zirconia-based ceramic membrane. The other authors focused on the characterization of the membrane support; X-ray fluorescence (XRF) was devoted to B.K., X-ray diffraction and FTIR were carried out by F.B.; Raman Spectroscopy by Y.O.; the SEM and the experimental part of filtration, as well as the discussion of all the results were carried out by N.D., M.C. and M.B. All authors have read and agreed to the published version of the manuscript.

**Funding:** This research received no external funding.

**Acknowledgments:** We would like to thank Farhat Bouzerara Lecturer at the University of Jijel for his help to realize the ceramic membrane.

**Conflicts of Interest:** The authors declare no conflict of interest.

#### References

1. Lee, S.-H.; Chung, K.-C.; Shin, M.-C.; Dong, J.-I.; Lee, H.-S.; Auh, K.H. Preparation of ceramic membrane and application to the crossflow microfiltration of soluble waste oil. *Mater. Lett.* **2002**, *52*, 266–271. [[CrossRef](#)]
2. Oh, H.K.; Takizawa, S.; Ohgaki, S.; Katayama, H.; Oguma, K.; Yu, M.J. Removal of organics and viruses using hybrid ceramic MF system without draining PAC. *Desalination* **2007**, *202*, 191–198. [[CrossRef](#)]
3. Emani, S.; Uppaluri, R.; Purkait, M.K. Preparation and characterization of low cost ceramic membranes for mosambi juice clarification. *Desalination* **2013**, *317*, 32–40. [[CrossRef](#)]
4. Bouazizi, A.; Saja, S.; Achiou, B.; Ouammou, M.; Calvo, J.L.; Aaddane, A.; Younssi, S.A. Elaboration and characterization of a new flat ceramic MF membrane made from natural Moroccan bentonite. Application to treatment of industrial wastewater. *Appl. Clay Sci.* **2016**, *132–133*, 33–40. [[CrossRef](#)]
5. Ghouil, B.; Harabi, A.; Bouzerara, F.; Boudaira, B.; Guechi, A.; Demir, M.M.; Figoli, A. Development and characterization of tubular composite ceramic membranes using natural alumino-silicates for microfiltration applications. *Mater. Charact.* **2015**, *103*, 18–27. [[CrossRef](#)]
6. Jana, S.; Purkait, M.K.; Mohanty, K. Preparation and Characterizations of Ceramic Microfiltration Membrane: Effect of Inorganic Precursors on Membrane Morphology. *Sep. Sci. Technol.* **2010**, *46*, 33–45. [[CrossRef](#)]
7. Verweij, H. Inorganic membranes. *Curr. Opin. Chem. Eng.* **2012**, *1*, 156–162. [[CrossRef](#)]
8. Ismail, A.F.; Chandra Khulbe, K.; Matsuura, T. *Gas Separation Membranes*; Springer International Publishing: Berlin/Heidelberg, Germany, 2015; ISBN 978-3-319-01094-6.
9. Weir, M. Fabrication, characterization and preliminary testing of all-inorganic ultrafiltration membranes composed entirely of a naturally occurring sepiolite clay mineral. *J. Membr. Sci.* **2001**, *182*, 41–50. [[CrossRef](#)]
10. Murray, H.H. Traditional and new applications for kaolin, smectite, and palygorskite: A general overview. *Appl. Clay Sci.* **2000**, *17*, 207–221. [[CrossRef](#)]
11. Bouzerara, F.; Harabi, A.; Ghouil, B.; Medjemem, N.; Boudaira, B.; Condom, S. Elaboration and Properties of Zirconia Microfiltration Membranes. *Procedia Eng.* **2012**, *33*, 278–284. [[CrossRef](#)]
12. Yousefi, V.; Mohebbi-Kalhari, D.; Samimi, A. Ceramic-based microbial fuel cells (MFCs): A review. *Int. J. Hydrogen Energy* **2017**, *42*, 1672–1690. [[CrossRef](#)]
13. Xing, W.-H. Ceramic Membranes. In *Membrane-Based Separations in Metallurgy*; Elsevier: Amsterdam, The Netherlands, 2017; pp. 357–370; ISBN 9780128034279.

14. Zhang, S.; Wang, R.; Zhang, S.; Li, G.; Zhang, Y. Treatment of wastewater containing oil using phosphorylated silica nanotubes (PSNTs)/polyvinylidene fluoride (PVDF) composite membrane. *Desalination* **2014**, *332*, 109–116. [[CrossRef](#)]
15. Kayvani Fard, A.; McKay, G.; Buekenhoudt, A.; Al Sulaiti, H.; Motmans, F.; Khraisheh, M.; Atieh, M. Inorganic Membranes: Preparation and Application for Water Treatment and Desalination. *Materials (Basel)* **2018**, *11*, 74. [[CrossRef](#)] [[PubMed](#)]
16. Das, B.; Chakrabarty, B.; Barkakati, P. Preparation and characterization of novel ceramic membranes for micro-filtration applications. *Ceram. Int.* **2016**, *42*, 14326–14333. [[CrossRef](#)]
17. Goh, P.S.; Ismail, A.F. A review on inorganic membranes for desalination and wastewater treatment. *Desalination* **2018**, *434*, 60–80. [[CrossRef](#)]
18. Suriyakumar, S.; Raja, M.; Angulakshmi, N.; Nahm, K.S.; Stephan, A.M. A flexible zirconium oxide based-ceramic membrane as a separator for lithium-ion batteries. *RSC Adv.* **2016**, *6*, 92020–92027. [[CrossRef](#)]
19. Wang, P. A pilot study of the treatment of waste rolling emulsion using zirconia microfiltration membranes. *J. Membr. Sci.* **2000**, *173*, 159–166. [[CrossRef](#)]
20. Zhou, J.; Chang, Q.; Wang, Y.; Wang, J.; Meng, G. Separation of stable oil–water emulsion by the hydrophilic nano-sized ZrO<sub>2</sub> modified Al<sub>2</sub>O<sub>3</sub> microfiltration membrane. *Sep. Purif. Technol.* **2010**, *75*, 243–248. [[CrossRef](#)]
21. Zhong, J.; Sun, X.; Wang, C. Treatment of oily wastewater produced from refinery processes using flocculation and ceramic membrane filtration. *Sep. Purif. Technol.* **2003**, *32*, 93–98. [[CrossRef](#)]
22. Kroll, S.; Treccani, L.; Rezwan, K.; Grathwohl, G. Development and characterisation of functionalised ceramic microtubes for bacteria filtration. *J. Membr. Sci.* **2010**, *365*, 447–455. [[CrossRef](#)]
23. Krajewski, S.R.; Kujawski, W.; Dijoux, F.; Picard, C.; Larbot, A. Grafting of ZrO<sub>2</sub> powder and ZrO<sub>2</sub> membrane by fluoroalkylsilanes. *Colloids Surf. A Physicochem. Eng. Asp.* **2004**, *243*, 43–47. [[CrossRef](#)]
24. Larbot, A.; Gazagnes, L.; Krajewski, S.; Bukowska, M.; Kujawski, W. Water desalination using ceramic membrane distillation. *Desalination* **2004**, *168*, 367–372. [[CrossRef](#)]
25. Kumar, R.V.; Ghoshal, A.K.; Pugazhenthii, G. Fabrication of zirconia composite membrane by in-situ hydrothermal technique and its application in separation of methyl orange. *Ecotoxicol. Environ. Saf.* **2015**, *121*, 73–79. [[CrossRef](#)]
26. Erdem, İ.; Çiftçioğlu, M.; Harsa, Ş. Separation of whey components by using ceramic composite membranes. *Desalination* **2006**, *189*, 87–91. [[CrossRef](#)]
27. Dey, S.; Bhattacharya, P.; Bandyopadhyay, S.; Roy, S.N.; Majumdar, S.; Sahoo, G.C. Single step preparation of zirconia ultrafiltration membrane over clay-alumina based multichannel ceramic support for wastewater treatment. *J. Membr. Sci. Res.* **2018**, *4*, 28–33.
28. Abdullayev, A.; Bekheet, M.F.; Hanaor, D.A.H.; Gurlo, A. Materials and applications for low-cost ceramic membranes. *Membranes (Basel)* **2019**, *9*, 105. [[CrossRef](#)]
29. Zenikheri, F.; Harabi, A.; Boudaira, B.; Bouzerara, F.; Guechi, A.; Barama, S.-E.; Foughali, L.; Karboua, N. Elaboration of porous gehlenite and anorthite based ceramics using low price raw materials. *Cerâmica* **2016**, *62*, 242–248. [[CrossRef](#)]
30. Kolli, M.; Hamidouche, M.; Fantozzi, G.; Chevalier, J. Elaboration and characterization of a refractory based on Algerian kaolin. *Ceram. Int.* **2007**, *33*, 1435–1443. [[CrossRef](#)]
31. Ouali, A.; Sahnoune, F.; Belhouchet, H.; Heraiz, M. Effect of CaO addition on the sintering behaviour of anorthite formed from kaolin and CaO. *Acta Phys. Pol. A* **2017**, *131*, 159–161. [[CrossRef](#)]
32. Mukasa-Tebandeke, I.Z.; Ssebuwufu, P.J.M.; Nyanzi, S.A.; Schumann, A.; Nyakairu, G.W.A.; Ntale, M.; Lugolobi, F. The Elemental, Mineralogical, IR, DTA and XRD Analyses Characterized Clays and Clay Minerals of Central and Eastern Uganda. *Adv. Mater. Phys. Chem.* **2015**, *5*, 67–86. [[CrossRef](#)]
33. Macías-Quiroga, I.F.; Giraldo-Gómez, G.I.; Sanabria-González, N.R. Characterization of Colombian Clay and Its Potential Use as Adsorbent. *Sci. World J.* **2018**, *2018*, 1–11. [[CrossRef](#)]
34. Hosseini, S.A.; Niaei, A.; Salari, D. Production of  $\gamma$ -Al<sub>2</sub>O<sub>3</sub> from Kaolin. *Open J. Phys. Chem.* **2011**, *1*, 23–27. [[CrossRef](#)]
35. Johnston, C.T.; Elzea Kogel, J.; Bish, D.L.; Kogure, T.; Murray, H.H. Low-temperature Ftir Study of Kaolin-Group Minerals. *Clays Clay Miner.* **2008**, *56*, 470–485. [[CrossRef](#)]
36. Saikia, B.J.; Parthasarathy, G.; Borah, R.R.; Borthakur, R. Raman and FTIR Spectroscopic Evaluation of Clay Minerals and Estimation of Metal Contaminations in Natural Deposition of Surface Sediments from Brahmaputra River. *Int. J. Geosci.* **2016**, *7*, 873–883. [[CrossRef](#)]

37. Chikhi, M.; Meniai, A.-H.; Balaska, F.; Bencheikh-Lehocine, M. Modeling of the Ultrafiltration of a Dextran T500 Solution in a Tubular Membrane Module. *Chem. Eng. Technol.* **2008**, *31*, 501–506. [[CrossRef](#)]
38. Bottino, A.; Capannelli, C.; Del Borghi, A.; Colombino, M.; Conio, O. Water treatment for drinking purpose: Ceramic microfiltration application. *Desalination* **2001**, *141*, 75–79. [[CrossRef](#)]



© 2020 by the authors. Licensee MDPI, Basel, Switzerland. This article is an open access article distributed under the terms and conditions of the Creative Commons Attribution (CC BY) license (<http://creativecommons.org/licenses/by/4.0/>).